# Structural Characterization of the Cytosolic Domain of Kidney Chloride/Bicarbonate Anion Exchanger 1 (kAE1)†

Allison J. Pang, Susan P. Bustos, and Reinhart A. F. Reithmeier*

*Department of Biochemistry, University of Toronto, 1 King's College Circle, Medical Sciences Building, Room 5216, Toronto, Ontario M5S 1A8, Canada*

*Received October 25, 2007; Revised Manuscript Received February 14, 2008*

ABSTRACT: Kidney anion exchanger 1 (kAE1) is a membrane glycoprotein expressed in α-intercalated cells in the collecting ducts of the kidney where it mediates electroneutral chloride/bicarbonate exchange. Human kAE1 is a truncated form of erythroid AE1 missing the first 65 residues of the N-terminal cytosolic domain, which includes a disordered acidic region (residues 1–54) and the first β-strand (residues 55–65) of the folded region. Unlike erythroid AE1, kAE1 does not bind deoxyhemoglobin, glycolytic enzymes, or cytoskeletal components. To understand the effect of the N-terminal deletion on the structure of the cytosolic domain, we performed an extensive biophysical analysis on $His_6$ tagged cytosolic domains of erythroid AE1 (cdAE1), kidney AE1 (cdkAE1), and a novel truncation mutant (cdΔ54AE1) missing the first 54 residues, but retaining the β-strand. Circular dichroism did not detect any major differences in secondary structure, and sedimentation analyses showed that all three proteins were dimeric. Differential scanning calorimetry revealed that cdAE1 and cdΔ54AE1 had similar thermal stabilities with midpoints of transition higher than cdkAE1. cdAE1 and cdΔ54AE1 underwent similar pH-dependent fluorescence changes, while cdkAE1 exhibited a higher intrinsic fluorescence at neutral and acidic pH. Urea denaturation resulted in dequenching of tryptophan fluorescence in cdAE1, while tryptophans in cdkAE1 were already dequenched in the native state. We conclude that the absence of the central β-strand in cdkAE1 results in a less stable and more open structure than cdAE1. This structural change, in addition to the loss of the acidic amino-terminal region, may account for the altered protein binding properties of kAE1.

Anion exchanger 1 (AE1[1]), also known as Band 3, is a major integral protein of the human erythrocyte membrane. It is a 911 amino acid glycoprotein that is responsible for the electroneutral exchange of bicarbonate for chloride (*1*). Human AE1 has a monomer molecular weight of 95 kDa and exists as a dimer and a tetramer in the red blood cell membrane (*2, 3*). Mild proteolytic cleavage of this protein in erythrocyte membranes yields two functional domains. The 52 kDa C-terminal transmembrane domain (Gly361−Val911) spans the membrane space 12–14 times (*4–7*) and mediates the anion transport function (*1, 8*). The 43 kDa N-terminal cytosolic domain includes Met1−Lys360 and provides binding sites for various red cell cytoskeletal and cytosolic proteins (*1*). The cytosolic domain of Band 3 (cdAE1) acts as an anchoring site for ankyrin and protein 4.2, both of which are found in the membrane's cytoskeleton (*9, 10*). Band 3 is therefore thought to play an important role in maintaining the shape, stability, and flexibility of the red blood cell (*11, 12*). Band 3 also binds and regulates the function of deoxyhemoglobin and various glycolytic enzymes such as glyceraldehyde-3-phosphate dehydrogenase, aldolase, and phosphofructokinase (*9, 13, 14*). The cytosolic domain is characterized by a highly acidic amino-terminal region with an N-acetylated terminal methionine (*15*). This region of the domain is involved in binding associated proteins (*9*), although other parts of the cytosolic domain also provide protein binding sites, such as the ankyrin-binding loop (*16*).

In erythrocytes, AE1 transports bicarbonate, which is produced by carbonic anhydrase, into the plasma in exchange for chloride, thereby increasing the $CO_2$-carrying capacity of the blood (*8*). In the human kidney, a truncated form of AE1 (kAE1) catalyzes the exchange of bicarbonate and chloride across the basolateral membrane of acid-secreting cells in the collecting ducts of the kidney, resulting in bicarbonate reabsorption into the blood and promoting acid excretion into the urine. Since kidney and erythroid AE1 are derived from the same gene, they are identical in primary sequence, except for the N-terminal domain of kAE1, which

† This work was funded by Grant FRN 15266 from the Canadian Institutes of Health Research. S.P.B. was supported by a Graduate Student Fellowship from the Canadian Blood Services and A.J.P. by a Life Sciences Summer Studentship.

* To whom correspondence should be addressed: Department of Biochemistry, University of Toronto, Room 5216 Medical Sciences Building, 1 King's College Circle, Toronto, ON M5S 1A8, Canada. Tel: (416) 978-7739. Fax: (416) 978-8548. E-mail:r.reithmeier@utoronto.ca.

[1] Abbreviations: $A_{600}$, absorbance at 600 nm; AE1, anion exchanger 1; BME, β-mercaptoethanol; CD, circular dichroism; cdAE1, cytosolic domain of erythroid AE1; cdΔ54AE1, cytosolic domain of AE1 missing the first 54 residues; cdkAE1, cytosolic domain of kidney AE1; Cp, specific heat capacity; DSC, differential scanning calorimetry; ILK, integrin-linked kinase, IPTG, isopropyl β-D-thiogalactopyranoside; kAE1, kidney anion exchanger 1; LB, Luria–Bertani; $MW_{app}$, apparent molecular weight; $MW_{seq}$, sequence molecular weight; Ni-NTA, nickel-nitrilotriacetic acid; PCR, polymerase chain reaction; pI, isoelectric point; PMSF, phenylmethanesulfonyl fluoride; rpm, revolutions per minute; SDS−PAGE, sodium dodecyl sulfate−polyacrylamide gel electrophoresis; $T_m$, midpoint of transition.

10.1021/bi702149b CCC: $40.75 
Published on Web 03/22/2008

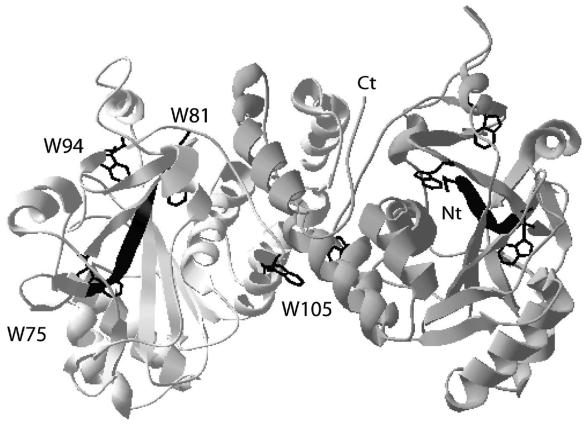


FIGURE 1: Crystal structure of the cytosolic domain of human AE1 (cdAE1). The structure of the cdAE1 dimer was solved at a resolution of 2.90 Å at pH 4.8. Both monomers are coloured gray and the $\beta$-strand insert, which is absent in the kidney isoform, is shown in black. The N-terminal residues 1–54 are not visible in the crystal structure. The positions of the tryptophan residues are shown in black. Reprinted with permission from ref 8. Copyright 1989 Wiley-Liss.

is missing residues 1–65 (*17*). Since the acidic residues of the amino-terminal region, which electrostatically bind cytoskeletal and cytosolic proteins, are absent in this protein, the cytosolic domain of kidney AE1 (cdkAE1) is thought to have a different function than the erythroid isoform, potentially mediating the binding of specific kidney proteins. Indeed, kAE1 has been shown not to bind to glycolytic enzymes, deoxyhemoglobin, protein 4.1, or ankyrin (*17, 18*), but has been found to bind to integrin-linked kinase (ILK), a protein involved in actin cytoskeletal interactions (*19*).

The crystal structure of erythroid cdAE1 has been elucidated (Figure 1) at low pH by X-ray diffraction, revealing a tight, symmetric dimer stabilized by interlocking dimerization arms contributed by each subunit (*20*). The purified recombinant protein has been shown (*15*) to have the same secondary structure, Stokes radius, and pH-dependent conformation changes as the native cytosolic domain prepared from red blood cells. Except for a missing N-acetylated amino-terminus, no significant differences were observed between the recombinant and native proteins. The first 54 residues of AE1 were unresolved in the crystal structure due to the strongly anionic and disordered nature of the region (*20, 21*). The crystal structure also shows that residues 55–65 in AE1 form a $\beta$-strand that is present in the core of the protein. Since the kidney isoform is missing this $\beta$-strand, it is possible that the kidney cytosolic domain has a significantly different structure from the full-length erythroid form. The goal of this work was to structurally analyze cdAE1 and cdkAE1, as well as a novel truncation mutant, cdΔ54AE1, which lacks the first 54 residues but retains the core $\beta$-strand. A schematic of these three constructs is illustrated in Figure 2. Various biophysical tools were employed to map out the structural differences between the three constructs. Our data show that the loss of the $\beta$-strand results in a less stable and more open structure for the cytosolic domain of kAE1. This structural change, in addition to the loss of the acidic amino-terminal region, could account for the inability of kAE1 to bind the same proteins as erythroid AE1. Furthermore, the altered structure of the cytosolic domain may allow kAE1 to interact with a unique set of proteins in kidney cells.

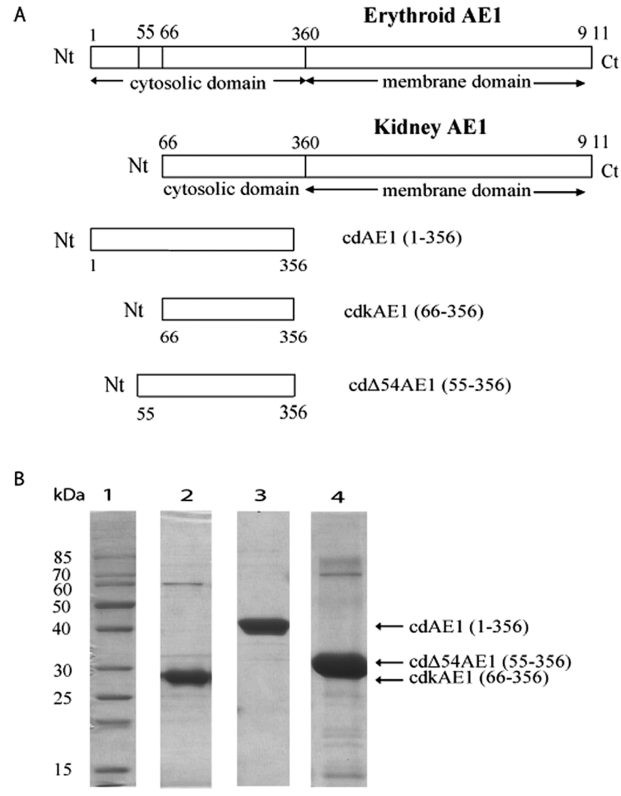


FIGURE 2: (A) Domain structure of AE1, kAE1, and the cdAE1, cdkAE1, and cdΔ54AE1 constructs. Residues 1–54 are not visible in the crystal structure, and residue 356 is the last residue that was visible in the crystal structure of cdAE1. Residues 55–65 encompass the first $\beta$-strand in cdAE1. (B) 12% SDS−PAGE gel of the purified constructs stained with Coomassie Blue. Lane 1: molecular weight markers. Lane 2: eluate of purified cdkAE1. Lane 3: eluate of purified cdAE1. Lane 4: eluate of purified cdΔ54AE1.

## MATERIALS AND METHODS

*Materials.* The following is a list of materials used and their suppliers: pcDNA3 vector (Invitrogen, San Diego, CA); mutagenic primers (ACGT Corp., Toronto, ON); pETBlue-1 vector and Tuner BL21(DE3)pLacI *Escherichia coli* competent cells (Novagen, Madison, WI); growth media for *E. coli* (BD, Sparks, MD); chloramphenicol and carbenicillin (Sigma, St. Louis, MO); isopropyl $\beta$-D-thiogalactopyranoside (Bioshop, Burlington, ON); $Ni^{2+}$-NTA agarose resin (QIAGEN, Germantown, MD); PD-10 gel filtration columns (Amersham Biosciences); lysozyme from chicken egg white (Sigma, St. Louis, MO); deoxyribonuclease from bovine pancreas (Sigma, St. Louis, MO); and Sequanal grade urea (Pierce, Rockford, IL).

*Plasmid Construction and Mutagenesis.* The cdAE1 construct was amplified by PCR from full-length human AE1 on a pcDNA3 vector, which was then cloned into a pETBlue-1 expression vector. This expression vector contained an IPTG-inducible T7 *lacO* promoter (*22*). The reverse primer encoded six histidine residues that were used as a carboxyl-terminal tag for purification purposes. cdkAE1 and cdΔ54AE1 were also amplified by PCR from full-length human AE1 using primers that corresponded to their respective amino- and carboxyl- termini. The primary sequence of all three proteins extended to the last visible residue in the crystal structure of cdAE1, which is serine 356. Constructs were confirmed by sequencing by ACGT Corp (Toronto, Canada).

*Protein Expression and Purification.* All constructs were expressed in *E. coli* Tuner BL21(DE3)pLacI competent cells at 37 °C. Large cultures of cells were grown in 1 L of LB medium containing 50 $\mu$g/mL carbenicillin and 34 $\mu$g/mL chloramphenicol until an $A_{600}$ of 0.5–0.6. Expression of the constructs was induced by the addition of 1 mM IPTG (*23*). Cells were grown for an additional five hours and then harvested by centrifugation at 4 000 rpm for 30 min. Cell pellets were solubilized in 80 mL of lysis buffer (50 mM sodium phosphate, 300 mM sodium chloride, 10 mM imidazole, 0.2% $\beta$ME, and 0.2% Triton X-100 (pH 8.0)). The following protease inhibitors were used: 2 $\mu$g/mL aprotinin, 1.6 mM PMSF, 0.7 $\mu$g/mL pepstatin A, and 10 $\mu$M leupeptin. DNase and lysozyme were added to the cell pellets. The solubilized cell pellets were sonicated at 40% duty for 1.5 min on ice. Purification of the protein constructs was carried out using 1 mL of $Ni^{2+}$-NTA agarose beads (QIAGEN) per 80 mL of lysate at 4 °C. Resin was equilibrated using the lysis buffer and, following protein binding, was washed twice with 10 mL of wash buffer (50 mM sodium phosphate, 300 mM sodium chloride, 20 mM imidazole, and 0.2% BME (pH8.0)). Protein was eluted three times using 1 mL of elution buffer (50 mM sodium phosphate, 300 mM sodium chloride, 250 mM imidazole, and 0.2% BME (pH8.0)). The three elution fractions were combined, filtered, and applied to a pre-equilibrated PD-10 gel filtration column in order to exchange the buffer with 10 mM $NH_4HCO_3$. Proteins were lyophilized overnight and stored at –20 °C. Protein purity was determined to be >95% by SDS−PAGE and Coomassie Blue staining. The final concentration of the purified proteins was measured by the BioRad protein assay, which is based on the Bradford assay.

*Analytical Ultracentrifugation.* Sedimentation equilibrium was performed on an Optima XL-A/XL-I analytical ultracentrifuge (Beckman Instruments, Palo Alto, CA) at 10 000, 13 000, 16 000 and 19 000 rpm at 20 °C. Samples were prepared by dissolving lyophilized protein in 10 mM sodium phosphate and 50 mM sodium chloride (pH 7.5). Sedimentation was carried out on cdAE1, cdkAE1, and cdΔ54AE1, each at three different concentrations with the corresponding $A_{280}$ values of 0.3, 0.6, and 1.0. Data analysis was performed using XL-A/XL-I software (Origin version 4.1) from Beckman Instruments.

Sedimentation velocity was also performed on an Optima XL-A/XL-I analytical ultracentrifuge (Beckman Instruments, Palo Alto, CA) at 30 000 rpm at 4 °C. Samples were prepared by dissolving lyophilized protein in 50 mM sodium phosphate and 100 mM sodium chloride (pH 7.5). Data analysis was performed using XL-A/XL-I software (SedFit and Ultrascan) from Beckman Instruments.

*Circular Dichroism.* Lyophilized protein was dissolved in buffer containing 50 mM sodium phosphate and 100 mM sodium chloride, and adjusted to either pH 5.0, 7.5, or 10.5. Samples were filtered through a 0.22 $\mu$m syringe filter. The final concentrations of the protein solutions are indicated in the figure captions. Circular dichroism was performed on a Jasco J-810 spectropolarimeter. All spectra were measured at 24 °C from 200 to 260 nm with a 1 nm data pitch in a 1 mm path length cell. The mean residue ellipticity was measured as a function of wavelength. The secondary structure content of the spectra was determined using the SELCON3 program from the CDPro software package.

*Differential Scanning Calorimetry.* Lyophilized protein was dissolved in buffer containing 50 mM sodium phosphate and 100 mM sodium chloride, and preadjusted to either pH 5.0, 7.5, or 10.5. Samples were filtered through a 0.22 $\mu$m syringe filter. The final concentrations of the protein solutions are indicated in the figure captions. Heat capacity measurements from 25 to 90 °C were obtained on a Microcal VP-DSC differential scanning calorimeter. Samples were heated at a rate of 1.5 °C/min. After subtracting the buffer blank, the heat capacity was plotted as a function of temperature. Origin 7.0 data analysis software was used to make baseline subtractions, which corrected the heat capacity differences between the native and denatured sates. It was also used to analyze temperature denaturation by fitting the data to an independent non-two-state transition model (*24*):

$$\mathrm{Cp}(T) = [K_A(T)\Delta H_{mA}/\{[1 + K_A(T)]^2 RT^2\} + ...$$

*pH Dependence of Intrinsic Fluorescence.* Stock solutions of each protein were made by dissolving lyophilized samples in 50 mM sodium phosphate and 100 mM sodium chloride (pH7.5) and by filtering them through a 0.22 $\mu$m syringe filter. The stock protein was then diluted 50 times into the same buffer preadjusted to the desired pH, ranging from pH 5.0 to pH 10.5 in 0.5 increments. The final concentration of the protein samples was ~0.1–0.2 mg/mL. Samples were equilibrated overnight at 4 °C and were allowed to reach room temperature prior to fluorescence measurement. The excitation wavelength was 290 nm, and the fluorescence emission was measured from 300 to 420 nm for each protein sample at each pH value. Measurements were taken at 24 °C by a Fluorolog-3 FL3-22 spectrofluorometer. Fluorescence intensity was plotted against wavelength for samples at pH 5.0, 7.5, and 10.5. The average emission wavelength (AEW) was also plotted as a function of pH. The AEW was calculated from each emission spectrum according to the equation $\sum$(wavelength × intensity)/$\sum$(intensity). Due to the asymmetry of the emission intensity spectra, the average emission wavelength, which is the intensity weighted average of all of the wavelengths scanned, was used instead of the maximum emission wavelength for greater accuracy (*25*).

*Urea Denaturation Measured by Intrinsic Fluorescence.* Stock solutions of cdAE1 and cdkAE1 were made by dissolving lyophilized samples in 50 mM sodium phosphate and 100 mM sodium chloride (pH 7.5) and filtering them through a 0.22 $\mu$m syringe filter. The stock protein was diluted 50 times into the same buffer preadjusted to the desired urea concentration ranging from 0 to 8 M. Samples were equilibrated overnight at 4 °C and were allowed to reach room temperature prior to fluorescence measurement. The excitation wavelength was 290 nm, and the fluorescence emission was measured from 300 to 420 nm for each protein sample at each urea concentration. Measurements were taken at 24 °C by a Fluorolog-3 FL3-22 spectrofluorometer. The maximum peak fluorescence intensity was plotted against urea concentration. The average emission wavelength was also plotted as a function of urea concentration.

## RESULTS

*1. Expression and Purification of cdAE1, cdkAE1, and cdΔ54AE1 Proteins.* The purification of $His_6$-tagged cdAE1, cdkAE1, and cdΔ54AE1 was performed by $Ni^{2+}$-affinity

Table 1: Summary of biophysical properties of cdAE1, cdkAE1, and cdΔ54AE1 at pH 7.5

| property | cdAE1 | cdΔ54AE1 | cdkAE1 |
|---|---|---|---|
| $MW_{app}/MW_{seq}$ oligomeric state (sedimentation equilibrium) | 1.83 dimer | 1.77 dimer | 1.93 dimer |
| $S_{20,w}$ (sedimentation velocity) | 4.1 S | 3.9 S | 3.7 S |
| secondary structure (circular dichroism) | % α-helix = 30.5 ± 1.2; $n = 3$ | % α-helix = 34.7 ± 1.8; $n = 3$ | % α-helix = 32.0 ± 0.5; $n = 3$ |
| midpoint of transition ($T_m$ (°C)) (calorimetry) | pH 5 = 73.7 ± 1.7; $n = 4$ | pH 5 = 73.1 ± 2.9; $n = 5$ | pH 5 = 62.4 ± 5.3; $n = 5$ |
| | pH 7.5 = 65.3 ± 1.2; $n = 12$ | pH 7.5 = 65.8 ± 1.2; $n = 11$ | pH 7.5 = 60.1 ± 2.2; $n = 11$ |
| | pH 10.5 = 56.1 ± 2.7; $n = 6$ | pH 10.5 = 56.0 ± 2.0; $n = 6$ | pH 10.5 = 50.7 ± 3.0; $n = 5$ |
| enthalpy[a] (kcal/mol) (calorimetry) | pH 5 = 341.2 ± 20.8; $n = 4$ | pH 5 = 305.0 ± 47.5; $n = 5$ | pH 5 = 213.6 ± 29.5; $n = 5$ |
| | pH 7.5 = 95.9 ± 14.1; $n = 9$ | pH 7.5 = 87.8 ± 11.6; $n = 9$ | pH 7.5 = 65.6 ± 14.0; $n = 8$ |
| | pH 10.5 = 60.5 ± 11.4; $n = 6$ | pH 10.5 = 55.0 ± 10.8; $n = 6$ | pH 10.5 = 45.2 ± 10.5; $n = 5$ |

[a] The enthalpy values are only estimates due to the fact that thermal denaturation was an irreversible process.

chromatography as described in Materials and Methods. This method of purification yielded approximately 15–20 mg of protein per liter of cell culture, the kidney isoform routinely having the highest expression. All three proteins were more than 95% pure as determined by SDS gel electrophoresis (Figure 2B), and they ran as monomers with molecular masses of roughly 43 kDa (cdAE1), 32 kDa (cdkAE1), and 35 kDa (cdΔ54AE1), with variable amounts of an upper dimer band. The predicted molecular weights of cdAE1, cdkAE1, and cdΔ54AE1, including their $His_6$ tag, are 40 866 Da, 33 269 Da, and 34 738.5 Da, respectively. The identities of the constructs were confirmed by mass spectrometry analysis, which gave molecular weights of 40 942 Da (cdAE1), 33 346 Da (cdkAE1), and 34 815 Da (cdΔ54AE1), all of which were ~76 Da higher than the predicted values. This extra molecular mass was most likely due to formation of a β-mercaptoethanol adduct (+76 Da) on one of the cysteine residues during purification.

*2. Analytical Ultracentrifugation: Sedimentation Equilibrium and Sedimentation Velocity of cdAE1, cdkAE1, and cdΔ54AE1 Proteins.* Sedimentation equilibrium analysis was carried out to determine the oligomeric state of the proteins and to see if the missing 65 (cdkAE1) or 54 residues (cdΔ54AE1) affect the dimerization of the cytosolic domain of AE1. It was previously shown by gel filtration, disulfide bond cross-linking experiments (*26*), and sedimentation equilibrium (*27*) that cdAE1 exists as a dimer in solution. It is predicted that the missing N-terminal residues of cdkAE1 and cdΔ54AE1 would not distort the native structure of the C-terminal dimerization arm. Sedimentation analysis indicated apparent molecular weights that were approximately twice those of their sequence molecular weights. The ratios of apparent molecular weight versus sequence molecular weight are listed in Table 1. The plots of ln(abs) versus the radius square were linear for all samples, indicating that the samples were primarily composed of one major species. A representative sedimentation plot of cdAE1 is shown in Figure 3, as well as the residuals from fitting the data to a single-ideal species model. The results show that the three proteins exist as stable dimers in solution.

Sedimentation velocity was carried out to compare the relative conformations of cdAE1, cdkAE1, and cdΔ54AE1 based on their $S_{20,w}$ values. The sedimentation coefficient of the erythroid cytosolic fragment has been previously estimated to be ~4.1 S (*26*), in agreement with our own result for this construct. cdkAE1 and cdΔ54AE1 had sedimentation values of 3.7 and 3.9 S, respectively. Smaller $S_{20,w}$ values

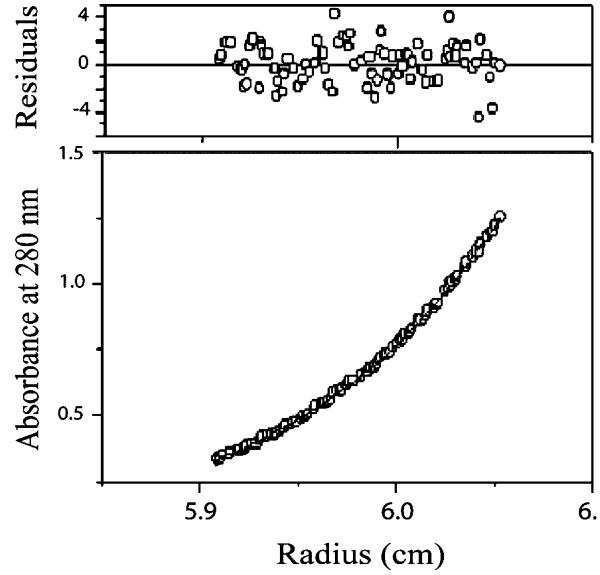


FIGURE 3: Sedimentation equilibrium of cdAE1. Absorbance at 280 nm is plotted as a function of the radius. The residuals from fitting the data to a single ideal species model are shown. The experiment was done at 20 °C at a speed of 13 000 rpm. The protein was dissolved in 50 mM sodium chloride and 10 mM sodium phosphate at pH 7.5.

indicated that the truncated proteins moved slower within the centrifugal force likely due to their lower molecular weights and perhaps more extended structures. Previous work using gel filtration has already reported the effect of pH on the shape of cdAE1 and cdkAE1 (*17*). These studies showed that both constructs reversibly elongate in a similar manner at alkaline pH.

*3. Secondary Structure Content of cdAE1, cdkAE1, and cdΔ54AE1: Analysis by Circular Dichroism Spectroscopy.* The secondary structures of cdAE1, cdkAE1, and cdΔ54AE1 were examined by circular dichroism (CD) spectroscopy. A representative spectrum of each protein at pH 7.5 is shown in Figure 4. A comparison of the CD spectra, however, revealed only minor variations in secondary structure content between the constructs. Each spectrum exhibited a negative maximum at 208 nm and a shoulder at 222 nm, which are dominating features of an α-helical protein. The helical content of cdAE1 based on its crystal structure was 26% (*20*). The deconvolution of the CD spectra revealed similar helical content between cdAE1, cdkAE1, and cdΔ54AE1 of approximately 30–35% α-helix (Table 1). Since the crystal structure of cdAE1 was elucidated at pH 4.8 (*20*), it was important to determine if the secondary structure differs at

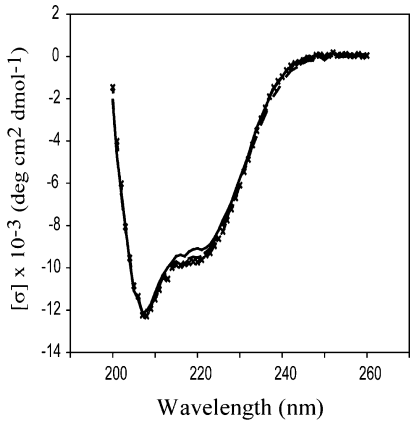


FIGURE 4: Circular dichroism spectra of purified cdAE1, cdkAE1, and cdΔ54AE1 at pH 7.5. Lyophilized proteins were dissolved in 100 mM sodium chloride and 50 mM sodium phosphate (pH 7.5) and scanned at 24 °C in a 1 mm cell in a Jasco J-810 spectropolarimeter. The final concentrations of cdAE1 (—), cdkAE1 (– – –), and cdΔ54AE1 (–×–), were 0.36 mg/mL, 0.38 mg/mL, and 0.34 mg/mL, respectively. The spectra are expressed as the mean residue ellipticity ($\sigma$) as a function of wavelength.

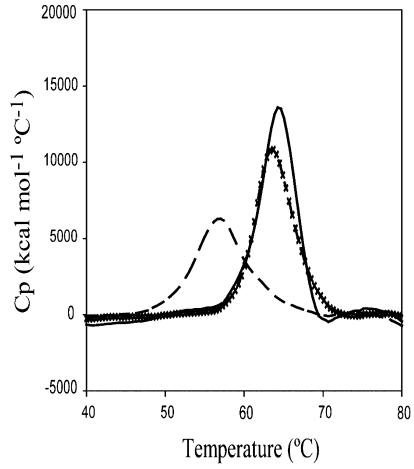


FIGURE 5: Thermal denaturation of purified cdAE1, cdkAE1, and cdΔ54AE1 by differential scanning calorimetry at pH 7.5. All DSC scans were baseline-subtracted. The proteins were dissolved in 100 mM sodium chloride and 50 mM sodium phosphate (pH 7.5) to final protein concentrations of 0.9 mg/mL (cdAE1, —), 1.2 mg/mL (cdkAE1, – – –), and 1.0 mg/mL (cdΔ54AE1, –×–). The specific heat capacity (Cp) was measured as the temperature was increased from 40 to 80 °C. No transition was observed once the proteins were thermally denatured, cooled, and reheated.

physiological and acidic conditions. For this reason, pH values of 5.0, 7.5, and 10.5 were used to detect possible pH-dependent structural changes. Based on previous fluorescence and gel filtration experiments, there is evidence that the global conformation of cdAE1 elongates as pH is increased (*26*). However, there were no changes detected in the CD spectrum of the three constructs at the different pH values tested, indicating that the secondary structural features were maintained.

*4. Thermal Denaturation of cdAE1, cdkAE1, and cdΔ54AE1 by Differential Scanning Calorimetry.* Calorimetry can detect major structural and stability changes in proteins, which appear as perturbations in the temperature of maximum heat capacity ($T_m$). Thermal denaturation by differential scanning calorimetry (DSC) was used to compare the thermal stability of the cdAE1, cdkAE1, and cdΔ54AE1 proteins. A representative plot of the thermal denaturation of cdAE1, cdkAE1, and cdΔ54AE1 at pH 7.5, as performed by DSC, is shown in Figure 5. It was found that cdkAE1 had the lowest $T_m$ (60 °C) and that cdAE1 (65 °C) and cdΔ54AE1 (66 °C) shared similar calorimetric characteristics. The results indicate that the thermal stability of cdAE1 was unaffected by removal of the disordered amino-terminal extension (residues 1–54) but was destabilized by removal of the core $\beta$-strand. The area under the curve is the enthalpy of denaturation ($\Delta H$). This thermodynamic value represents the contributions of van der Waals forces, hydrogen bonds and salt bridges to the stability of the folded protein (*28*). Cooling and reheating of the samples revealed an irreversible thermal denaturation. While $\Delta H$ values calculated from irreversible processes may not correspond precisely to the native and denatured unfolding equilibrium, the reported $\Delta H$ values (Table 1) are still useful in comparing protein stabilities. cdkAE1 had a smaller enthalpy than both cdAE1 and cdΔ54AE1, indicating a lower stability. At low pH, all constructs adopted more stable conformations with higher enthalpies, and at high pH, they became less stable with markedly lower enthalpies.

It was also observed that the thermal stability of the three proteins was pH-dependent, being the least stable at alkaline pH and the most stable at acidic pH. The effect of pH on the $T_m$ values of cdAE1, cdkAE1, and cdΔ54AE1 is recorded in Table 1. cdAE1 and cdΔ54AE1 behaved similarly, while cdkAE1 had a lower $T_m$ at all pH values. These observations corresponded with other studies that have reported the $T_m$ of cdAE1 to be pH-dependent with a value of 67 °C at pH 7.51 (*26*). It was also noticed that the peaks at low pH were broader, most likely due to aggregation of the samples. This may be explained by the fact that at pH 5.0, the proteins approach their isoelectric points, the pI of cdAE1, cdkAE1, and cdΔ54AE1 being 4.70, 5.29, and 5.30, respectively. These thermal denaturation studies show that the $\beta$-strand plays a structural role in the stabilization of the cytosolic domain. Furthermore, the cytosolic domains containing the $\beta$-strand are the most stable at low pH. cdkAE1 has only a slightly higher midpoint of transition at pH 5 than at neutral pH, suggesting that it is less well packed under acidic conditions compared to cdAE1.

*5. Effect of pH on the Intrinsic Fluorescence of cdAE1, cdkAE1, and cdΔ54AE1.* Differences in tertiary structure between cdAE1, cdkAE1, and cdΔ54AE1 were further studied by carrying out intrinsic tryptophan fluorescence studies. It has been previously shown that cdAE1 undergoes a pH-dependent conformational change, characterized by a dramatic increase in tryptophan fluorescence at alkaline pH (*26*) and an expansion of its Stokes radius (*15*). Since a cluster of four tryptophan residues is located C-terminal to the 65 residue amino extension, the local environment of these tryptophans in cdkAE1 may differ from that of cdAE1, and the tryptophans would therefore exhibit different fluorescence properties and sensitivities toward pH titration. As the pH increased, cdAE1, cdkAE1, and cdΔ54AE1 experienced an increase in fluorescence intensity due to dequenching of their tryptophan residues (Figure 6). cdAE1 and the novel mutant cdΔ54AE1 both showed a similar increase in intensity, doubling in value from pH 5 to 10.5. At acidic and neutral pH, however, cdkAE1 exhibited a higher intrinsic

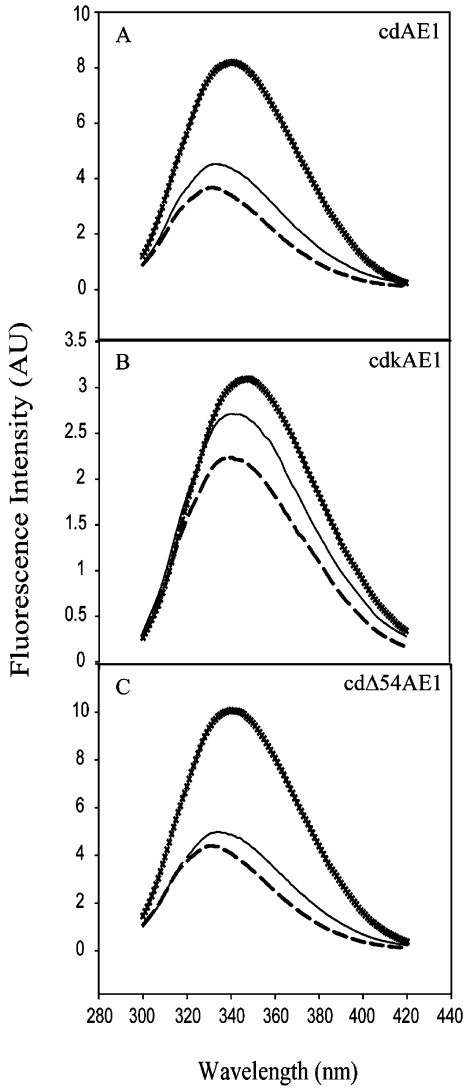


FIGURE 6: Intrinsic tryptophan fluorescence emission spectra of (A) cdAE1, (B) cdkAE1, and (C) cdΔ54AE1 at pH values 5.31 (− − −), 7.48 (−), and 10.04 (−×−) . The intensity is plotted as a function of wavelength. Lyophilized proteins were dissolved in 100 mM sodium chloride and 50 mM sodium phosphate preadjusted to the desired pH. The intrinsic fluorescence emission was measured from 300 to 420 nm following excitation at 290 nm.

fluorescence than cdAE1, which suggests that it has a more open structure under these conditions compared to the cdAE1 protein.

Figure 7 is a representative plot of the average emission wavelength (AEW) of all three proteins as a function of pH. A red-shift in peak wavelength at alkaline pH was observed, indicating that the tryptophans were becoming exposed to a more polar environment. Even at neutral pH the fluorescence spectrum of cdkAE1 was more red-shifted, indicating a higher degree of exposure of tryptophans to a more polar environment. At alkaline pH, the three constructs exhibited similar fluorescence properties, consistent with a similar exposure of tryptophans to solvent.

*6. Urea Denaturation of cdAE1 and cdkAE1 by Intrinsic Tryptophan Fluorescence.* Urea denaturation was used to examine the stability of cdAE1 and cdkAE1, and to further understand the consequence of truncating the N-terminus of AE1's cytosolic domain. The observed fluorescence emission intensity of cdAE1 peaked at 4 M urea due to the dequenching of its tryptophans. This increase was then followed by a decrease in intensity at higher urea concentrations due to further exposure of the Trp residues to the aqueous solvent. The urea denaturation profile of cdΔ54AE1 was similar to the erythroid construct (data not shown). In contrast, cdkAE1displayed a higher intrinsic fluorescence under native conditions and a continual decrease in fluorescence as urea increased. Both constructs, however, eventually denatured to a similar unfolded state as seen by the convergence of their fluorescence intensities at 6 M urea.

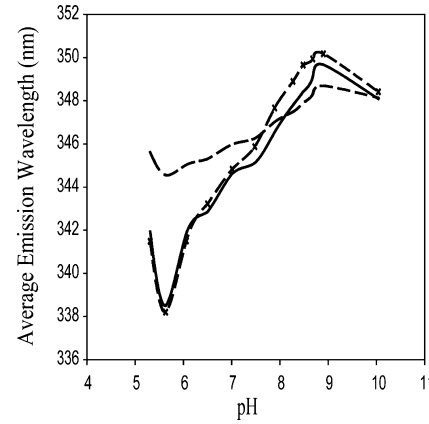


FIGURE 7: Intrinsic tryptophan fluorescence intensity of purified cdAE1 (−), cdkAE1 (− − −), and cdΔ54AE1 (−×−). The average emission wavelength is plotted as a function of pH. Lyophilized proteins were dissolved in 100 mM sodium chloride and 50 mM sodium phosphate preadjusted to the desired pH. The intrinsic fluorescence emission was measured from 300 to 420 nm following excitation at 290 nm.

The average emission wavelength red-shifted as the amount of urea increased (Figure 8B). This observed red-shift indicated that the tryptophans were progressively becoming exposed to a more polar environment. As shown in Figure 8B, cdAE1 and cdkAE1 underwent similar conformational changes; however, cdkAE1 was less resistant to urea at lower concentrations of the denaturant.

## DISCUSSION

In this study, the biophysical properties of cdAE1, cdkAE1, and the novel mutant cdΔ54AE1 were compared to determine the effect of loss of the central $\beta$-strand on the structure and stability of the cytosolic domain. As shown by sedimentation equilibrium, removal of residues 1–65 had no effect on the dimerization of the cytosolic domain of AE1, indicating that cdkAE1 was still able to retain a dimeric structure in solution. Circular dichroism analysis showed that the amino-truncations (either Δ1–65 or Δ1–54) did not have a significant effect on the secondary structure content of the cytosolic domain. The loss of the short $\beta$-strand alone (residues 55–65) would not be expected to produce dramatic changes in the CD spectrum.

Differential scanning calorimetry compared the thermal stability of cdkAE1 to that of cdAE1. cdkAE1 consistently had lower $T_m$ values regardless of the pH, indicating a less stable structure. The calorimetric values of the novel mutant cdΔ54AE1 were similar to those of cdAE1, strengthening the contention that the $\beta$-strand (residues 55–65) helps stabilize the cytosolic domain of AE1. These results were predicted because the crystal structure of AE1 shows that the $\beta$-strand is located within the core of the domain. When

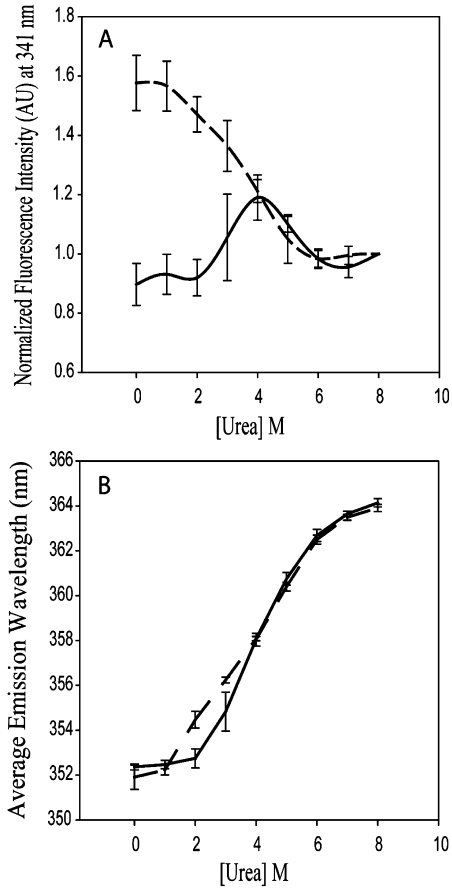


FIGURE 8: Urea denaturation of cdAE1 (−) and cdkAE1 (− − −) monitored by intrinsic tryptophan fluorescence. Lyophilized proteins were dissolved in 100 mM sodium chloride and 50 mM sodium phosphate preadjusted to the desired urea concentration. The intrinsic fluorescence intensity was measured from 300 to 420 nm following excitation at 290 nm. The vertical bars represent the standard deviation; $n = 4$. (A) Intrinsic fluorescence emission intensity of the proteins at 341 nm is plotted as a function of urea concentration. (B) Average emission wavelength was calculated from each spectrum and plotted as a function of urea concentration.

the $\beta$-strand was removed, as in cdkAE1, there was a significant effect on the $T_m$. As expected, removal of residues 1–54 did not alter the stability of the domain as these residues form a flexible extension that was not resolved by X-ray crystallography. Previous studies (*27*) showed that point mutations in cdAE1 that cause hereditary spherocytosis had little or no effect on the stability of the cytosolic domain, in contrast to the destabilization caused by the loss of the $\beta$-strand in cdkAE1.

Varying the pH had a noticeable effect on the thermal stability of all three proteins. At acidic pH, the $T_m$ value increased compared to neutral and alkaline pH. This indicated that the proteins acquired a greater thermal stability at low pH, perhaps adopting a more compact conformation as revealed by the crystal structure. cdkAE1 was always the least stable at all pH values; however, the difference in $T_m$ was greatest (~10 °C) at low pH.

The intrinsic fluorescence of a folded protein is primarily dependent on the local environment of its tryptophans (*29*). Normally, when tryptophan is exposed to a hydrophobic environment, the fluorescence emission is of high intensity and is blue-shifted. Upon exposure to a more polar environment, tryptophan fluorescence decreases and its emission spectrum experiences a red-shift (*29*). However, this is often not the case for multitryptophan proteins, such as cdAE1 where the tryptophans are found at residues 75, 81, 94, and 105. At alkaline pH, the fluorescence intensity of cdAE1 increased and there was a red-shift in average emission wavelength. These observations indicated that an opening of the structure had occurred, thereby dequenching fluorescence and exposing the tryptophan residues to a more polar environment.

Both cdAE1 and cdΔ54AE1 underwent similar pH-dependent conformational changes, indicating structural similarity. cdkAE1 was not as structurally sensitive to pH titration as were the other two protein constructs because of its more open structure at low pH. In comparison, cdAE1 and the novel mutant had a more compact and folded structure at low pH, and gradually adopted a more open conformation as pH increased. Although the secondary structure content between the three proteins is comparable, the intrinsic fluorescence data suggest that cdkAE1 has a less compact structure, especially at low pH.

Intrinsic fluorescence was also used as a probe for the urea denaturation experiments, once again revealing information about the local environment of the N-terminal tryptophan cluster (*29*). The tryptophans of cdAE1 first become dequenched, and then quenched at higher urea concentrations. During denaturation, the tryptophans in cdAE1 move away from quenching residues and become dequenched, but as the protein continues to denature, the tryptophans become further exposed to the more polar, aqueous environment, which in return causes a decrease in fluorescence (*29*). Under native conditions, the intrinsic fluorescence of cdkAE1 was high, indicating that the tryptophan residues were dequenched. The tryptophans in this construct would already be more apart from quenching residues so that denaturation would only cause the tryptophans to become even more exposed to the solvent, hence the decrease in fluorescence that was observed. By 6 M urea, the fluorescence intensity of both cdAE1 and cdkAE1 converge and plateau, indicating a similar unfolded state.

In conclusion, the biophysical techniques employed in this study were useful in structurally characterizing the cytosolic domain of the kidney $Cl^-/HCO_3^-$ anion exchanger 1. It was shown through sedimentation equilibrium and circular dichroism experiments that cdkAE1 retains a dimeric structure and has secondary structure content similar to that of the erythroid isoform. The analyses made by sedimentation velocity, DSC, and intrinsic tryptophan fluorescence experiments established that removal of the acidic amino-terminal extension (residues 1–54 only) had little effect on the folding and stability of cdAE1, whereas deletion of the $\beta$-strand (residues 55–65), as in cdkAE1, produced a less stable and more open structure.

The crystal structure of the cytosolic domain of AE1 has been elucidated for the erythroid isoform in acidic conditions. In addition, the structure of the central compact region of cdAE1 at neutral pH has been found to be indistinguishable from the crystal structure, as investigated by site-directed spin labeling and electron paramagnetic resonance (*21*). We plan to further characterize the structure of cdkAE1 by X-ray crystallography or NMR analysis. Based on the results presented in this study, NMR would perhaps be the most amenable technique for solving the structure of cdkAE1, which seems to adopt a less compact and a more open

structure. NMR is also an ideal technique for studying the dynamic behavior of cdkAE1 versus cdAE1. Another potential project could also include a molecular dynamics simulation. Starting with the geometry of the known cdAE1, it would be interesting to see if removal of the first beta strand (residues 55–65) could then generate a hypothetical, stable structure.

By comparison to cdAE1, the deletion of residues 1–65 has two effects on the cytosolic domain: (1) the loss of the acidic amino-terminal extension that is involved in binding associated proteins, and (2) the loss of the $\beta$-strand causing changes to the structure and stability of the domain. Both of these effects could account for the inability of kAE1 to bind cytoskeletal proteins and glycolytic enzymes. Indeed, the loss of the $\beta$-strand could have long-range effects on the structure of the cytosolic domain. The changes in the structure of cdkAE1 may also allow kAE1 to interact with different proteins compared with AE1. In order to fully understand the function and regulation of kAE1 it would be important to identify its interacting protein partners in kidney cells.

## ACKNOWLEDGMENT

Jing Li is thanked for the construction of the cdAE1, cdkAE1, and cdΔ54AE1 vectors. We also thank Walid Houry for the use of the fluorescence and circular dichroism spectrophotometers, David Clarke for the use of the differential scanning calorimeter, and Rongmin Zhao for the ultracentrifugation analyses.

## REFERENCES

1. Lepke, S., and Passow, H. (1976) Effects of incorporated trypsin on anion exchange and membrane proteins in human red blood cell ghosts. *Biochim. Biophys. Acta 455*, 353–370.
2. Wang, D., Kühlbrandt, W., Sarabia, V. E., and Reithmeier, R. A. F. (1993) Two-dimensional structure of the membrane domain of human Band 3 the anion transport protein of the erythrocyte membrane. *EMBO J. 12*, 2233–2239.
3. Casey, J. R., and Reithmeier, R. A. F. (1991) Analysis of the Oligomeric State of Band 3 the Anion Transport Protein of the Human Erythrocyte Membrane, by Size Exclusion High Performance Liquid Chromatography. *J. Biol. Chem. 266*, 15726–15737.
4. Reithmeier, R. A. F., Chan, S. L., and Popov, M. (1996) Structure of the Erythrocyte Band 3 Exchanger, in *Handbook of Biological Physics* (Konings, W. N., Kaback, H. R., and Lolkema, J. S., Eds.) pp 281–309, Elsevier Science B.V., Amsterdam.
5. Fujinaga, J., Tang, X.-B., and Casey, J. R. (1999) Topology of the Membrane Domain of Human Erythrocyte Anion Exchange Protein, AE1. *J. Biol. Chem. 274*, 6626–6633.
6. Popov, M., Li, J., and Reithmeier, R. A. F. (1999) Transmembrane folding of the human erythrocyte anion exchanger (AE1, Band 3) determined by scanning and insertional N-glycosylation mutagenesis. *Biochem. J. 339*, 269–279.
7. Zhu, Q., Lee, D. W. K., and Casey, J. R. (2003) Novel Topology in C-terminal Region of the Human Plasma Membrane Anion Exchanger, AE1. *J. Biol. Chem. 278*, 3112–3120.
8. Jennings, M. L. (1989) Structure and function of the red blood cell anion exchange protein. *Pro.g Clin. Biol. Res. 292*, 327–338.
9. Perrotta, S., Borriello, A., Scaloni, A., De Franceschi, L., Brunati, A. N., Turrini, F., Nigro, V., del Giudice, E. M., Nobili, B., Conte, M. L., Rossi, F., Lolascon, A., Donella-Deana, A., Zappia, V., Poggi, V., Anong, W., Low, P., Mohandas, N., and Della Ragione, F. (2005) The N-terminal 11 amino acids of human erythrocyte band 3 are critical for aldolase binding and protein phosphorylation: implications for band 3 function. *Blood 106*, 4359–4366.
10. Hargreaves, W. R., Giedd, K. N., and Branton, D. (1980) Reassociation of ankyrin with band 3 in erythrocyte membranes and in lipid vesicles. *J. Biol. Chem. 255*, 11965–11972.
11. Lux, S. E., and Palek, J. (1995) Disorders of the red cell membrane, in *Blood: Principles and Practice of Hematology*, Lippincott, Philadelphia.
12. Peters, L. L., Shivdasani, R. A., Liu, S. C., Hanspal, M., John, K. M., Gonzalez, J. M., Brugnara, C., Gwynn, B., Mohandas, N., Alper, S. L., Orkin, S. H., and Lux, S. E. (1996) Anion Exchanger 1 (Band 3) is Required to Prevent Erythrocyte Membrane Surface Loss but Not to Form the Membrane Skeleton. *Cell 86*, 917–927.
13. Walder, J. A., Chatterjee, R., Steck, T. L., Low, P. S., Musso, G. F., Kaiser, E. T., Rogers, P. H., and Arnone, A. (1984) The Interaction of Hemoglobin with the Cytoplasmic Domain of Band 3 of the Human Erythrocyte Membrane. *J. Biol. Chem. 259*, 10238–10246.
14. Low, P. (1986) Structure and function of the cytoplasmic domain of band 3: Center of erythrocyte membrane-peripheral protein interactions. *Biochim. Biophys. Acta 864*, 145–167.
15. Wang, C. C., Badylak, J. A., Lux, S. E., Moriyama, R., Dixon, J. E., and Low, P. S. (1992) Expression, purification, and characterization of the functional dimeric cytoplasmic domain of human erythrocyte band 3 in Escherichia coli. *Protein Sci. 1*, 1206–1214.
16. Chang, S. H., and Low, P. S. (2003) Identification of a Critical Ankyrin-binding Loop on the Cytoplasmic Domain of Erythrocyte Membrane Band 3 by Crystal Structure Analysis and Site-directed Mutagenesis. *J. Biol. Chem. 278*, 6879–6884.
17. Wang, C. C., Moriyama, R., Lombardo, C. R., and Low, P. S. (1995) Partial Characterization of the Cytoplasmic Domain of Human Kidney Band 3. *J. Biol. Chem. 270*, 17892–17897.
18. Ding, Y., Casey, J. R., and Kopito, R. R. (1994) The Major Kidney AE1 Isoform Does Not Bind Ankyrin (ANK1) in Vitro. *J. Biol. Chem. 269*, 32201–32208.
19. Keskanokwong, T., Shandro, H. J., Johnson, D. E., Kittanakom, S., Vilas, G. L., Thorner, P., Reithmeier, R. A. F., Akkarapatumwong, V., Yenchitsomanus, P., and Casey, J. R. (2007) Interaction of Integrin-linked Kinase with the Kidney Chloride/Bicarbonate Exchanger, kAE1. *J. Biol. Chem. 282*, 23205–23218.
20. Zhang, D., Kiyatkin, A., Bolin, J. T., and Low, P. S. (2000) Crystallographic structure and functional interpretation of the cytoplasmic domain of erythrocyte membrane band 3. *Blood 96*, 2925–2933.
21. Zhou, Z., DeSensi, S. C., Stein, R. A., Brandon, S., Dixit, M., McArdle, E. J., Warren, E. M., Kroh, H. K., Song, L., Cobb, C. E., Hustedt, E. J., and Beth, A. H. (2005) Solution Structure of the Cytoplasmic Domain of Erythrocyte Membrane Band 3 Determined by Site-Directed Spin Labeling. *Biochemistry 44*, 15115–15128.
22. Giordano, T. J., Deuschle, U., Bujard, H., and McAllister, W. T. (1989) Regulation of coliphage T3 and T7 RNA polymerases by the lac repressor-operator system. *Gene 84*, 209–219.
23. Studier, F. W., and Moffatt, B. A. (1986) Use of bacteriophage T7 RNA polymerase to direct selective high-level expression of cloned genes. *J. Mol. Biol. 189*, 113–130.
24. *DSC Data Analysis in Origin*, Tutorial Guide, MicroCal LLC, Northampton, MA, 2002.
25. Shirley, B. A. (1995) *Protein Stability and Folding: Theory and Practice*, Humana Press, Totowa.
26. Appell, K. C., and Low, P. S. (1981) Partial Structural Characterization of the Cytoplasmic Domain of the Erythrocyte Membrane Protein, Band 3. *J. Biol. Chem. 256*, 11104–11111.
27. Bustos, S. P., and Reithmeier, R. A. F. (2006) Structure and Stability of Hereditary Spherocytosis Mutants of the Cytosolic Domain of the Erythrocyte Anion Exchanger 1 Protein. *Biochemistry 45*, 1026–1034.
28. Schulz, G. E., and Schirmer, R. H. (1979) *Principles of Protein Structure*, Springer-Verlag New York Inc., New York.
29. Lakowicz, J. R. (1999) *Principles of Fluorescence Spectroscopy*, 2nd ed., Kluwer Academic/Plenum Publishers, New York.

BI702149B